Petroleum Science (2019) 16:527–540
https://doi.org/10.1007/s12182-019-0313-y

ORIGINAL PAPER

Geochemical characteristics of the Permian marine mudstone and constraints on its provenance and paleoenvironment in the Fenghai area, Fujian Province, southeastern China

Qi-Feng Xie[1,2] · Yuan-Feng Cai[3] · Yun-Peng Dong[1] · Ming-Guo Zhai[1,4] · Dun-Peng Li[2]

Received: 26 April 2018 / Published online: 11 May 2019

Abstract

Permian marine strata have gradually become a research focus in the world. The marine strata of the Late Permian Dalong Formation (P_3d) in the Fenghai area, Fujian Province, have become more and more important as their geochemical characteristics record important geological information and are a good indicator for recovering and reconstructing the paleo-sedimentary environments and tectonic attributes. The major elements, trace elements and rare earth elements were analyzed by XRF and ICP-MS, respectively. Based on the results of detailed field geological surveys, profile measurements as well as typical sample collection, the tectonic setting and provenance of Permian marine mudstone were comprehensively discussed. The results showed that the Dalong Formation (P_3d) was deposited in an active continental margin tectonic environment as revealed by the relation between $Fe_2O_3 + MgO$ and TiO_2 and Al_2O_3/SiO_2. The fingerprint characteristics of Mn, Fe, Co, Ni and REE and the ratio of U/Th, V/Cr, Sr/Ba, $(La/Yb)_N$ and $V/(V + Ni)$ indicated that the sedimentary provenance was mainly derived from potassium feldspar, followed by muscovite. Sedimentary water bodies showed a gradually decreasing depositional rate trend, water depth gradually shallowing and paleo-salinity and productivity gradually increasing. Moreover, since transient delamination occurred during sedimentary processes, sedimentary water bodies showed obvious neritic characteristics. It was consistent with the results revealed by lithological and geochemical characteristics. Calcareous mudstone and siltstone transitioned into fine sandstone from bottom to top, indicating paleo-water bodies became shallow. The research results provided good reference and guidance for understanding Permian paleo-sedimentary environments and tectonic attributes of the Yong'an area, Fujian Province, southeastern China.

Keywords Late Permian · Dalong Formation · Geochemistry · Sedimentary characteristic · Tectonic environment

1 Introduction

In recent years, along with the deepening and strengthening of the research on the marine sedimentary strata in China and abroad, the marine sedimentary strata in Fujian Province have also gradually become a focus for concern (Hu et al. 2011; Xie et al. 2012; Duan 2013; Liu et al. 2014).

With the development and improvement in measuring techniques and analytical methods, the major element and trace element (including rare earth) compositions have been widely used for understanding provenance, tectonic setting and paleo-sedimentary environment (Zhang and Zhang 2006; Yang et al. 2014; Xie et al. 2015a, b; Hu et al. 2017a, b; Tang et al. 2017; Cao et al. 2018). The Si, Th, Sc, Zr and Hf in sediments have stable chemical properties during weathering, transportation, deposition and digenesis. These are often used as important parameters for analyzing

Edited by Jie Hao

✉ Qi-Feng Xie
xieqf@fzu.edu.cn

✉ Yuan-Feng Cai
Caiyf@nju.edu.cn

1 State Key Laboratory of Continental Dynamics, Northwest University, Xi'an 710069, Shaanxi, China

2 College of Zijin Mining, Fuzhou University, Fuzhou 350108, Fujian, China

3 State Key Laboratory for Mineral Deposits Research, Nanjing University, Nanjing 210046, Jiangsu, China

4 Institute of Geology and Geophysics, Chinese Academy of Sciences, Beijing 100029, China

provenance attributes and discriminating tectonic settings. Their main controlling factor was provenance (Boulter et al. 2004; Cao et al. 2007).

Furthermore, V, Cr, Ni, Co and U were active elements in sediments and their content reflected their physical and chemical properties, even the influence of paleo-sedimentary environment and tectonic setting during their formation (Xie et al. 2015a; Gao et al. 2017). The geochemical indexes and ratios of these elements can be used to analyze provenance attributes and discriminate tectonic settings (Tang et al. 2017). Therefore, it is of great significance to research the ratios of geochemical elements and their variations.

Permian marine strata were widely deposited in the Fenghai region, Fujian Province, southeastern China. However, there has been little study on the strata due to limited data. The study of Permian marine strata was of great significance to understand provenance attributes and sedimentary environments. Therefore, in this paper, the geochemical characteristics of the mudstone of the Dalong Formation (P_3d) were analyzed in order to discuss the geological significance of the Permian. The results laid a solid foundation for research into the Permian marine strata of China and can also be used to guide the research and exploration direction of the Permian strata in Fujian Province.

2 Geological overview

2.1 Overview of stratigraphic development

The Fenghai area is located in An'sha town of Longyan City, Fujian Province. It is in the middle reaches of the Jiulong stream, 44 km away to the northwest of Yong'an City, and Yong'an city is located in west-central Fujian Province. Structurally, the Fenghai area is located in the southwest part of the southwest Fujian depression, to the west of the intersection of the NEE-trending Ninghua–Nanping fault zone and the NNE-trending Zhenghe–Dapu fault zone. There are two NW-trending major faults and several NE-trending secondary faults. Permian strata are composed of neritic carbonates of the Lower Permian Qixia Formation (P_1q), the interbedded limestone, dolomitic limestone, mudstone and siliceous rocks of the Wenbishan Formation (P_1w) and neritic mudstones and shales of the Tongziyan Formation (P_1t). The Tongziyan Formation (P_1t) is dominated by fine clastic rocks of marine–continental transitional facies, containing coal measure strata. It is divided into two parts. The lower part is composed of fine sandstone, siltstone and mudstone, containing coal seams, and the upper part is the main coal-bearing strata of Fujian Province. The Middle Permian consists of the Cuipingshan Formation (P_2cp), which is divided into upper, middle and lower lithological sections. It is dominated by fine clastics of alluvial and lacustrine facies, such as sandstone, siltstone and mudstone; The Late Permian consists of the Dalong Formation (P_3d), which is dominated by calcareous and siliceous mudstone deposits of neritic–littoral facies. The lower part is calcareous siltstone and mudstone, and the middle and upper parts are marlstone, mudstone and carbonaceous siltstone. The tectonic division, survey section and sampling locations are shown in Fig. 1a–c, respectively.

2.2 Description of profile section

The P_3d marine sedimentary section is located to the southwest of Fenghai Hydropower Station, Xiaohuo Village, Longyan City, Fujian Province (Fig. 1b). The section has a length of 700 m and elevation of 195 m. The coordinate is 26°00′48.3″N, 117°12′31.0″E at the starting point and 26°01′01.7″N, 117°12′23.3″E at the end point (Fig. 2).

The specific development of the lithological section is shown in Fig. 2. According to lithological characteristics, 28 layers were observed. The Late Permian Dalong Formation was divided into three sections. The lower part is dominated by gray medium-thin argillaceous siltstone and interbedded with medium-thin gray mudstone and dark gray carbonaceous mudstone, light grayish and yellow silty mudstone. The middle part is dominated by medium-thin grayish yellow siltstone and interbedded with grayish purple thin calcareous siltstone and thin gray mudstone. The upper part is dominated by medium-thin siltstone and interbedded with medium-thin mudstone and carbonaceous mudstone (Fig. 2).

The boundary of the lithological section has clear contact with the underlying medium-thick grayish yellow medium sandstone of the upper part of the Middle Permian Cuipingshan Formation (P_2cp^3) in a parallel unconformity, overlying brownish red thin-bedded silty mudstone and grayish yellow argillaceous siltstone of the Triassic Xikou Formation (T_1x) in a fault unconformity (Fig. 2).

2.3 Sample collection and analyses

The section of the Dalong Formation (P_3d) is 2 km away from the northwest part of the Fenghai Hydropower Station. Dark gray mudstone or carbonaceous mudstone was selected for typical samples. The dark gray mudstone was located in No. 2 and 22 layers (Fig. 2a, e), light gray mudstone was located in No. 3, 5 and 24 layers and dark gray carbonaceous mudstone was located in No. 9, 12, 19 and 27 layers (Fig. 2b–d, f). In order to reduce the influence of surface weathering, unweathered samples were selected (Fig. 2). The weathering surface was removed with a geological hammer. Before the samples were selected and crushed, the weathering surface and relatively loose material were removed with a knife. Then, the samples were washed repeatedly with distilled water. Afterward, samples around 50 g were weighed

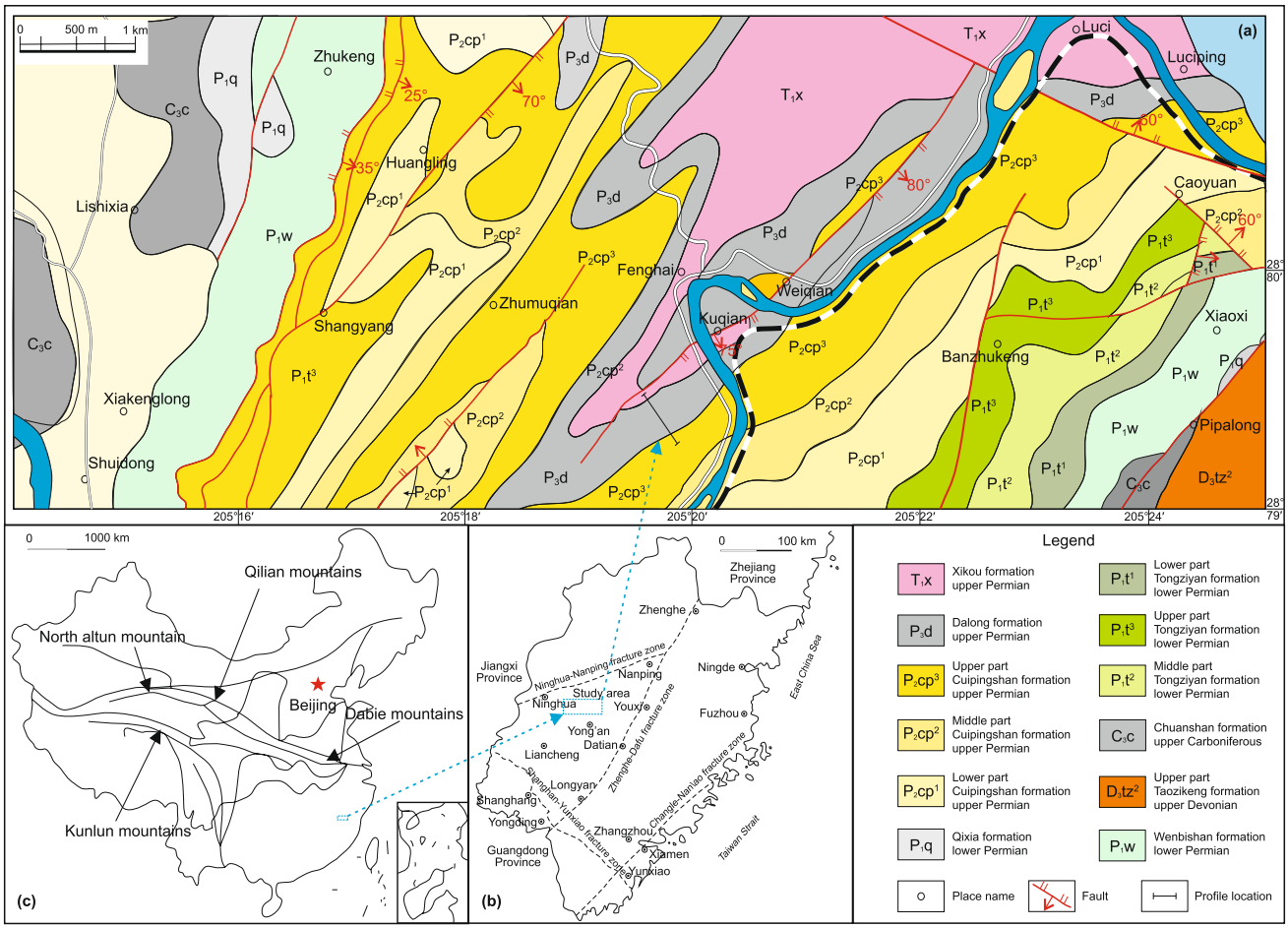

Fig. 1 Structural units division and stratigraphic distribution in the Fenghai area, Fujian Province

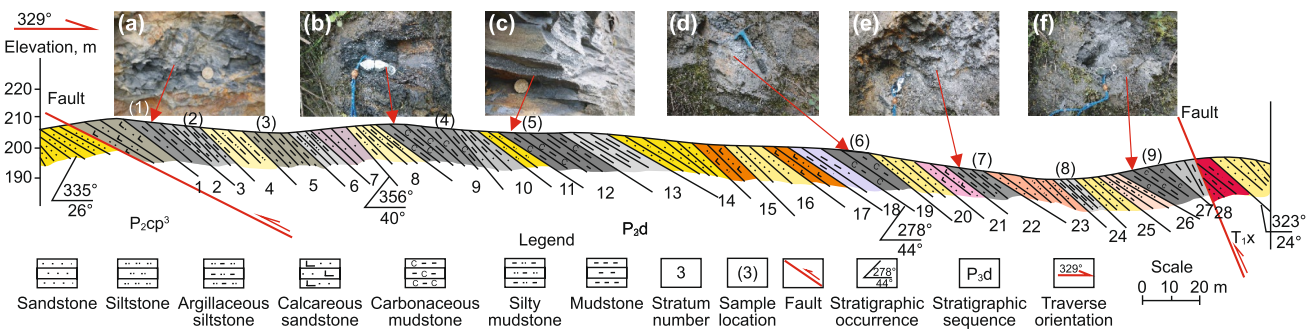

Fig. 2 Measured stratigraphic section of the Dalong Formation (P_3d) in the southeast part of the Fenghai Hydropower Station, Fujian Province

and pulverized to 200 mesh in an agate grinding bowl. The specific analysis process is from Xie et al. (2015a, b). Each sample was packed in paper with its number on it.

The samples were tested with a Thermo ARL 9800XP$^+$ X-ray fluorescence spectrometer in the State Key Laboratory for Mineral Deposits Research, Nanjing University. The trace elements, including Be, Bi, Cs, Cu, Ga, Li, Hf, Nb, Ni, Sc, Th, Ta, U and W, and rare earth elements were analyzed by inductively coupled plasma mass spectrometry (ICP-MS) (Cui et al. 2017; Xie et al. 2017). In order to ensure the accuracy and reliability of the test data, a master sample and duplicate samples were used for data quality monitoring and later inspection. The detection limit was less than or equal to 2 ppm (the elements of Ba, Cr, Rb, Sr and V with a detection

limit of less than or equal to 5 ppm were not included). The specific analysis process is shown in Han et al. (2016).

3 Geochemical composition and characteristics of marine mudstone

3.1 Characteristics of major elements

The geochemical characteristics of the major elements, trace elements and rare earth elements in sandstone and mudstone could reflect the variation of paleo-sedimentary environments, which are of great significance for indicating the tectonic setting and provenance (Bhatia 1983; Cox et al. 1995; Yu et al. 2014; Gao et al. 2017). The contents or ratios of major elements are often used to discuss the variation of sediment environments, the reduction and oxidation conditions of sedimentary water bodies, the distance between sedimentary water bodies and the shore and the variation of salinity (Ferguson et al. 2008; Xie et al. 2015a, b; Gao et al. 2017).

As shown in Table 1, the mean contents of Al_2O_3, SiO_2 and K_2O were 21.0%, 64.7% and 2.91%. The values of Post-Archean Australian Shale (PAAS) were lower than the mean content of Al_2O_3 and SiO_2 (McLennan 1989), higher than the content of K_2O and far higher than the content of CaO. SiO_2 mainly occurred in acidic granite, and its content was higher than PAAS, indicating the provenance was dominated by acidic granite with a high silica content. The Al and K were mainly derived from feldspar and clay minerals, such as kaolinite and illite (Cox et al. 1995). The enrichment of Al_2O_3 and depletion of K_2O indicated the source of feldspar was abundant, which was consistent with the results of the SiO_2–Al_2O_3 diagram. The provenance was mainly from plagioclase, potash feldspar and illite (Fig. 3). The high value of SiO_2 and Al_2O_3 indicated the distance from provenance was great (Gao et al. 2017). The content and ratio of Mn and Fe indicated a paleo-ocean sedimentary environment. The enrichment in Fe revealed a littoral–neritic sea or nearshore sedimentary environment. Mn was more stable than Fe, revealing abysmal sea or infra-littoral sedimentary environment. The contents of Fe_2O_3 and MnO were lower than PAAS, and particularly, the content of MnO was far below the PAAS (McLennan 1989), suggesting a littoral–neritic sea or nearshore sedimentary environment. The content of CaO was closely related to carbonate sediments, while MgO was mainly derived from basic igneous rocks. The content of CaO and MgO was far below the PAAS (McLennan 1989), revealing the depletion of carbonate sediment and basic igneous rocks. The content of SiO_2 also revealed the provenance was derived from granite. The value of K_2O/Na_2O is often regarded as the criterion to evaluate the salinity of sedimentary water bodies. The higher value corresponded to higher salinity (Jiao et al. 2004; Gao et al. 2017). The value of K_2O/Na_2O in the study area was between 3.9 and 10.3, showing an increasing trend, which reflected the salinity of paleo-water bodies increased. Moreover, the value of Al_2O_3/MgO and Mg/Ca also showed similar characteristics.

The Harker diagram revealed that content of Al_2O_3 presented an obvious negative correlation with SiO_2 and P_2O_5, but weak negative correlation with CaO and MgO (Fig. 4). The result indicated that with the increase in Al content, Si and P elements were absent and the content of Mg and Ca slightly decreased. It could be concluded that the reason why Al_2O_3 was enriched was other compositions, such as Si, P, Mg and Ca elements, were lost during diagenesis (Zhang et al. 2015; Han et al. 2016). Al_2O_3, K_2O, Na_2O and TiO_2 represented positive correlation, indicating that they were similar oxides and coeval deposits. There was no obvious correlation between the contents of Al_2O_3 and ΣREE.

3.2 Composition and characteristics of trace elements

The characteristics of trace elements and their variation are of great indicative significance to reconstruct paleo-sedimentary environments, such as the offshore distance, salinity, depth, the condition of oxidation–reduction, and to further understand tectonic setting, structural attributes and evolutionary processes. From the coast to abyssal sea during depositional process, Fe family elements, such as Fe, Cr, V and Ge, were enriched first. Then, elements such as Al, Ti, Zr, Ga, Nb and Ta were enriched, and finally, thiophilic elements, such as Pb, Zn, Cu and As, were enriched. Mn family elements, such as Mn, Co, Ni and Mo, tended to enrich in abyssal environments. The trace elements, such as Cr, Br, Ag, Cd, Mn, Cu, Co and Ba, also tended to enrich in abysmal environments (Bhatia and Crook 1986). Trace elements, such as Cr, Ni, V, and Ba, are easily absorbed by clay minerals. Therefore, the content of clay minerals can indirectly indicate the paleo-water depth, since it increased with the increase in water depth and offshore distance. Ba is closely related to the biological flux of overlying water in paleo-water bodies, so it can be used to estimate paleo-productivity (McManus et al. 1998; Pfeifer et al. 2001; Wagerich and Neuhuber 2005). The enrichment of V, Cr, Co, Ni, Cu, Zn, Cd and U which have similar characteristics to Ba was controlled by the oxidation–reduction characteristics of bottom seawater, sediments and pore water. This can be used to trace the oxidation–reduction status of bottom water in the paleoenvironment (Gardner et al. 1980; Tribovillard et al. 2006). The sulfophilic elements, such as Co, Ni, Cu, Zn and Cd, were deposited and enriched in the form of sulfides. Under the weak oxidation environment, Co and Ni were captured by the oxides of Mn and Fe and enriched (Shaw et al. 1990, 2011).

Table 1 Major element contents (%) and element ratios of mudstone in Fenghai area, Fujian Province

Sample ID	Component content, %											Ratio of component content					
	Al_2O_3	CaO	Fe_2O_3	K_2O	MgO	MnO	Na_2O	P_2O_5	TiO_2	SiO_2	LOI	K_2O/Al_2O_3	Al_2O_3/TiO_2	MgO/CaO	MnO/TiO_2	f_{CIA}	b
16-FH-01	25.87	0.07	1.07	3.36	0.42	0.01	0.64	0.05	0.82	61.49	6.16	0.13	31.49	5.94	0.01	86.42	1.61
16-FH-02	27.09	0.03	0.99	3.67	0.44	0.01	0.63	0.05	0.85	60.34	5.90	0.14	31.97	12.47	0.01	86.20	1.61
16-FH-03	26.43	0.03	1.22	1.04	0.15	0.01	0.30	0.03	0.89	63.34	6.35	0.04	29.60	4.79	0.00	95.08	0.55
16-FH-04	17.58	0.21	1.43	2.14	0.34	0.01	0.42	0.38	0.78	71.83	4.59	0.12	22.50	1.61	0.01	86.43	1.91
16-FH-05	19.30	0.12	0.84	2.19	0.23	0.01	0.50	0.07	0.86	64.06	11.61	0.11	22.41	1.95	0.01	87.30	1.18
16-FH-06	19.40	0.44	4.96	2.64	0.94	0.10	0.33	0.29	0.87	64.41	5.50	0.14	22.17	2.13	0.11	85.05	4.83
16-FH-07	22.80	0.04	1.40	2.99	0.32	0.01	0.57	0.06	0.78	65.04	5.70	0.13	29.06	8.78	0.01	86.39	1.38
16-FH-08	20.80	0.05	3.49	2.97	0.47	0.01	0.45	0.09	0.87	65.24	5.50	0.14	24.01	9.63	0.01	85.71	2.24
16-FH-09	20.25	0.06	4.06	3.05	0.91	0.01	0.33	0.11	0.98	64.64	5.49	0.15	20.75	14.13	0.01	85.46	4.47
16-FH-10	22.20	0.07	0.81	3.08	0.35	0.01	0.59	0.03	0.94	67.08	4.51	0.14	23.63	4.88	0.01	85.56	1.55
16-FH-11	12.61	0.05	3.04	2.21	0.41	0.01	0.35	0.05	0.78	74.75	5.28	0.18	16.26	8.26	0.01	82.84	3.27
16-FH-12	15.38	0.02	4.98	3.37	0.39	0.01	0.48	0.03	0.85	64.05	10.38	0.22	18.10	22.00	0.01	79.90	2.53
16-FH-13	23.80	0.05	1.42	5.15	0.50	0.01	0.75	0.18	1.42	54.38	11.90	0.22	16.73	9.41	0.01	79.99	2.08
Average value	21.04	0.10	2.29	2.91	0.45	0.01	0.49	0.11	0.90	64.67							
PAAS	18.88	1.29	7.18	3.68	2.19	0.11	1.19	0.16	0.99	62.40							

Dimensions: computing method of the content of CaO and Na_2O (when the mole content of CaO higher than Na_2O, select Na_2O, otherwise select CaO)

f_{CIA} (chemical alteration index) $= [Al_2O_3/(Al_2O_3 + CaO^* + Na_2O + K_2O)] \times 100$. PAAS is Australian Post-Archean Standard Shale

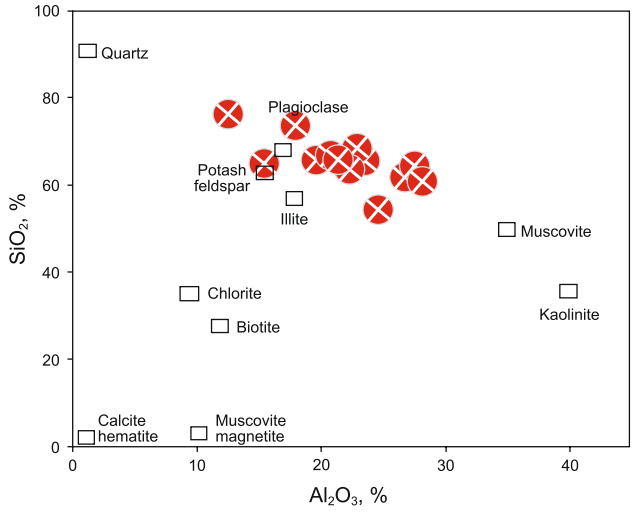

Fig. 3 Major element diagram of the Permian Dalong Formation mudstones in the Fenghai area, Fujian Province

to indicate the oxidation–reduction state of the sedimentary environment. The ratios of V/Cr, U/Th and Ni/Co were greater than 4.25, 1.25 and 7.0, respectively, indicating the oxidizing and anaerobic environments (Hatch and Leventhal 1992). However, the ratios of V/Cr, U/Th and Ni/Co were less than 2.50, 0.75 and 5.0, respectively, representing an oxidizing environment. The ratio was between the two representing a moderate oxidation–reduction environment (Beek et al. 2003; Hu et al. 2017a, b, c). The ratios of U/Th, V/Cr and Ni/Co were 0.22–0.29, 0.83–2.19 and 1.00–15.92, and the mean values were 0.48, 1.65 and 6.38, respectively, in the study area, which represented an oxidizing environment. The existence of the three abnormally high values of Ni/Co revealed an abrupt change occurred in the paleo-water body during the sedimentary process. The ratio of V/(V + Ni) was less than 0.6, reflecting paleo-water bodies were in an anoxic environment with weak delamination. The ratio of V/(V + Ni) was greater than 0.84, reflecting paleo-water bodies were in a reducing environment with strong delamination,

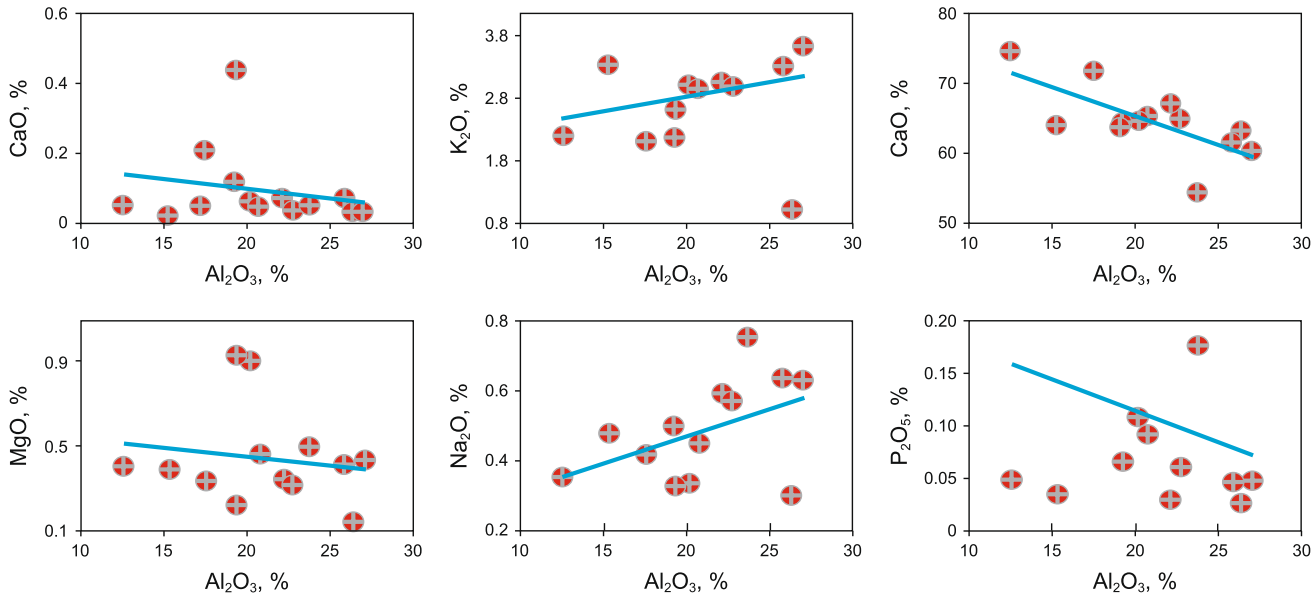

Fig. 4 Harker diagram of marine mudstone in the Fenghai area

The ratio of trace elements is commonly used to determine the variation of the paleo-seawater depth. The content of Ba element increased with the absorption on clay minerals, while the content of Sr remained stable or slightly decreased. Therefore, the ratio of Sr/Ba decreased with a gradual increase in paleo-water depth, which could be used to determine the depth of the paleo-seawater and the offshore distance. A Sr/Ba ratio of 10–0.6 represents low salinity water, less than 0.6 represented medium salinity water and more than 10 represented high salinity water (Zheng and Liu 1999). The ratio of V/Cr, U/Th and Ni/Co could also be used as shown in No. 22 layer. The ratio of Cu/Zn also changed with oxygen fugacity. A ratio of Cu/Zn greater than 0.63 indicates an oxidizing environment, 0.50–0.63 indicates a weakly oxidizing environment and less than 0.21 indicates a reducing environment, as shown in the No. 23 layer.

The trace elements of the marine mudstone of the Permian Dalong Formation in Fenghai region are shown in Table 2. The test results showed that the values of Mn, Ni, Co, Zn, Ba, Cr and V were in the ranges of 6×10^{-6}–594×10^{-6}, 9×10^{-6}–55×10^{-6}, 1×10^{-6}–54×10^{-6},

Table 2 Trace element contents (ppm) and ratios of mudstone in the Fenghai area

Sample ID	Li	Be	Sc	Ti	V	Cr	Mn	Co	Ni	Cu	Zn	Ga	Rb	Sr	Y	Zr	Nb	Mo	Sn
16-FH-01	164.6	2.9	3.0	3611.0	162.4	75.4	24.6	53.5	53.6	58.9	97.6	22.8	178.6	80.8	8.3	145.8	2.7	0.6	4.1
16-FH-02	202.0	2.4	8.1	4732.9	174.8	79.9	25.6	4.3	54.9	26.5	22.6	25.5	198.6	94.4	16.5	146.0	17.2	0.4	4.8
16-FH-03	169.5	1.5	4.2	4709.7	119.4	56.4	5.8	4.8	39.1	25.2	15.0	11.5	53.4	48.2	8.8	159.8	18.6	1.4	3.5
16-FH-04	55.6	2.5	3.2	4325.7	107.8	101.7	19.6	2.0	21.8	24.7	20.4	16.2	117.2	72.4	17.4	216.0	16.5	1.4	3.5
16-FH-05	143.7	7.8	5.9	4790.5	120.6	83.2	15.4	12.8	19.4	132.9	19.3	19.7	140.4	95.9	18.2	188.2	19.0	1.6	3.8
16-FH-06	63.6	3.1	12.8	5253.0	136.0	89.6	593.8	13.7	38.6	35.3	124.2	22.5	142.5	73.7	26.7	169.4	19.3	0.9	3.7
16-FH-07	98.1	3.2	9.1	4418.0	145.0	89.2	16.6	5.5	45.0	31.5	31.4	22.7	181.9	104.1	40.8	176.8	16.8	0.8	4.1
16-FH-08	54.6	2.9	6.4	4963.2	141.4	73.6	23.7	3.6	31.5	35.7	45.4	22.7	160.1	82.6	17.0	160.3	18.1	0.5	3.9
16-FH-09	34.0	2.6	9.1	5833.9	144.1	80.2	69.0	11.4	41.2	24.1	52.2	24.3	155.1	78.9	31.4	192.0	21.6	0.8	4.0
16-FH-10	131.7	2.3	8.1	5204.8	131.8	79.0	16.4	1.4	22.9	11.3	13.9	22.1	174.9	99.2	18.3	186.6	18.1	0.6	4.2
16-FH-11	13.3	1.9	5.2	4418.9	89.0	106.8	46.1	8.3	17.4	14.1	24.6	18.6	106.0	74.1	18.8	231.0	17.1	2.9	2.9
16-FH-12	7.7	2.4	9.0	4910.6	104.5	92.2	51.9	8.3	15.9	15.8	15.7	24.7	160.2	95.5	21.5	177.1	18.4	2.7	3.2
16-FH-13	1.8	4.5	7.7	8262.4	219.1	110.1	24.8	1.7	9.0	18.1	13.1	43.2	226.8	333.1	39.0	306.1	27.7	1.3	6.0

Sample ID	Cs	Ba	Hf	Ta	W	Pb	B	Th	U	Co/Th	La/Sc	Th/Sc	Th/Cr	Sr/Cu	B/Ga	Zr/Y	V/(V+Ni)	V/Ni	Sr/Ba
16-FH-01	28.7	431.4	4.7	0.0	0.2	51.7	0.8	6.4	5.9	8.4	0.0	2.1	0.1	1.4	0.0	17.6	0.8	3.0	0.2
16-FH-02	30.1	493.6	4.8	1.6	1.9	29.2	0.8	12.3	7.1	0.4	0.2	1.5	0.2	3.6	0.0	8.8	0.8	3.2	0.2
16-FH-03	11.0	167.0	5.7	1.6	1.9	27.7	0.8	10.0	5.9	0.5	0.4	2.4	0.2	1.9	0.1	18.2	0.8	3.1	0.3
16-FH-04	17.2	294.4	6.9	1.5	1.8	47.3	0.6	8.1	7.1	0.3	0.5	2.5	0.1	2.9	0.0	12.4	0.8	4.9	0.3
16-FH-05	26.5	347.6	5.9	1.6	5.1	66.1	0.8	13.0	7.7	1.0	0.3	2.2	0.2	0.7	0.0	10.3	0.9	6.2	0.3
16-FH-06	15.7	394.9	5.4	1.7	1.9	35.9	0.6	19.8	4.3	0.7	0.1	1.6	0.2	2.1	0.0	6.3	0.8	3.5	0.2
16-FH-007	25.6	434.4	5.5	1.4	2.9	42.9	1.0	13.0	8.1	0.4	0.2	1.4	0.2	3.3	0.1	4.3	0.8	3.2	0.2
16-FH-08	17.9	414.9	5.0	1.5	1.7	26.6	0.5	12.1	4.8	0.3	0.2	1.9	0.2	2.3	0.0	9.5	0.8	4.5	0.2
16-FH-09	14.5	462.5	6.2	1.9	4.7	34.2	0.6	18.6	4.7	0.6	0.2	2.0	0.2	3.3	0.0	6.1	0.8	3.5	0.2
16-FH-10	21.4	414.8	6.1	1.5	1.7	29.6	0.4	14.2	4.5	0.1	0.2	1.8	0.2	8.8	0.0	10.2	0.9	5.8	0.2
16-FH-11	8.5	350.7	7.0	1.5	86.9	39.5	0.4	11.6	3.9	0.7	0.3	2.2	0.1	5.3	0.0	12.3	0.8	5.1	0.2
16-FH-12	13.1	493.7	5.7	1.6	1.9	45.8	0.5	14.5	3.9	0.6	0.2	1.6	0.2	6.0	0.0	8.3	0.9	6.6	0.2
16-FH-13	16.0	906.4	8.8	2.0	2.5	121.8	1.7	23.4	7.9	0.1	0.3	3.0	0.2	18.4	0.0	7.9	1.0	24.3	0.4

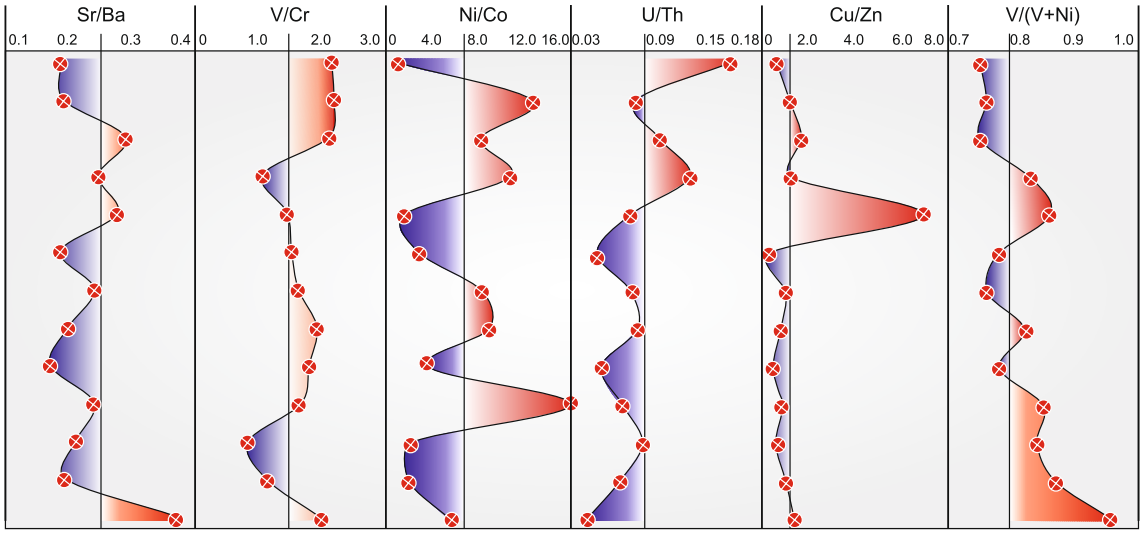

Fig. 5 Vertical variation of trace elements of the Permian Dalong Formation mudstone in the Fenghai area

13×10^{-6}–124×10^{-6}, 167×10^{-6}–494×10^{-6}, 56×10^{-6}–110×10^{-6} and 89×10^{-6}–219×10^{-6}, respectively, with mean values of 72×10^{-6}, 32×10^{-6}, 10×10^{-6}, 38×10^{-6}, 431×10^{-6}, 86×10^{-6} and 138×10^{-6}. The ratio of V/Ni was in the range of 3.0–24.3, with a mean value of 5.9, indicating the water bodies gradually became shallow. The ratio of Sr/Ba was between 0.17 and 0.37, with the mean value of 0.23, indicating the paleo-water bodies were in a weakly oxidizing environment (Fig. 4). The content of these elements in the mudstone of the Dalong Formation (P_3d) revealed the environment was weakly oxidizing and the paleo-sea depth gradually becoming shallow.

The ratio of Fe/Mn and Mg/Ca could reveal paleo-environment details. A high value represents a humid climate, and a low value represents an arid climate (Shaw et al. 1990, 2011; Ferguson et al. 2008). The ratio of Fe/Mn was in the range of 5.8–148, with a mean value of 53, showing an increasing trend. The ratio of Mg/Ca was in the range of 1.4–16.4, with a mean value of 6.9, and the median was 6.7. The ratio of Fe/Mn and Mg/Ca showed an increasing trend, indicating the paleo-environment changed from aridity to humidity.

The ratios of V/Cr, Ni/Co and U/Th were in the ranges of 3.03–6.58, 1.00–15.9 and 0.04–0.16, respectively, with mean values of 1.65, 6.38 and 0.08, revealing an oxidizing paleo-environment. At the same time, the ratio of V/(V + Ni) was in the range of 0.75–0.96, with a mean value of 0.82, higher than 0.84 at the top, revealing the Dalong Formation (P_3d) was in static oxidizing environment at a late stage and paleo-water bodies were in a strongly stratified state (Fig. 5). The content of Ba was in the range of 167×10^{-6}–906×10^{-6}, with a mean value of 431×10^{-6}, showing an increasing trend, which indicated the productivity of paleo-ocean had increased. The ratios of Sr/Ba, Mo/Al and Ba/Al are good indicators to evaluate paleo-productivity. They were in the ranges of 0.17–0.37, 0.03–0.45 and 11.9–71, with mean values of 0.23, 0.13, 40, respectively, revealing the productivity of the paleo-water body was low. The ratio of Cu/Zn was in the range of 0.28–6.90, with the mean value of 1.37, showing an increasing trend, which indicated a strongly oxidizing state (Fig. 5).

3.3 Composition and characteristics of rare earth elements

Rare earth elements (REE) have low concentrations in nature and are stable in hypergene environments. They are always regarded as the indicators of provenance. The content of rare earth elements (REE) was extremely low in seawater, but increased with the increase in water depth and could be used as an indicator of paleo-water depth (Dubini 2004; Wright et al. 1987). The differentiation characteristics between light rare earth element (LREE), heavy rare earth elements, Ce and Eu, and other elements in rare earth elements were changed accompanied with the transformation of the sedimentary environment, which can be used to reveal the oxidation–reduction environment. This phenomenon was prominent in paleo-sedimentary environments (Feng et al. 1997).

Ce^{3+} is dissolved and depleted in reducing water, but is enriched in oxidizing water (Elderfield 1988). Since the residence time of suspended particles and clastics can be ascertained from the differentiation of rare earth element (REE), $(La/Yb)_N$ could be used as the indicator of deposition rate. A low value represents a high deposition rate (Li et al. 2008).

The content of the rare earth elements in the Dalong Formation is shown in Table 3. The total content of rare

Table 3 REE contents (ppm) and element ratios of mudstone in Fenghai area, Fujian Province

Sample ID	La	Ce	Pr	Nd	Sm	Eu	Gd	Tb	Dy	Ho	Er	Tm	Yb	Lu	Y	ΣREE	LREE/HREE	$(La/Yb)_N$	δEu	δCe
16-FH-01	17.2	32.1	3.2	11.2	2.0	0.4	1.8	0.3	1.5	0.3	0.9	0.2	0.9	0.1	8.3	72.1	11.3	13.0	0.7	1.0
16-FH-02	39.0	68.3	7.6	25.2	4.5	0.9	3.9	0.6	3.0	0.6	1.8	0.3	1.9	0.3	16.5	157.6	11.9	14.3	0.6	0.9
16-FH-03	13.4	23.5	2.7	9.4	1.8	0.3	1.7	0.3	1.6	0.4	1.0	0.2	1.3	0.2	8.8	57.5	7.9	7.0	0.6	0.9
16-FH-04	20.8	41.8	4.4	16.9	4.1	0.8	4.6	0.7	4.0	0.8	1.7	0.3	1.8	0.3	17.4	103.0	6.3	7.8	0.6	1.0
16-FH-05	33.3	61.8	7.7	27.1	4.6	0.8	3.8	0.6	3.0	0.7	1.9	0.3	2.1	0.3	18.2	147.9	10.7	11.0	0.6	0.9
16-FH-06	48.5	88.0	10.3	36.1	6.9	1.5	6.0	0.9	4.9	1.0	2.7	0.5	3.0	0.5	26.7	210.7	9.9	10.8	0.7	0.9
16-FH-07	52.0	98.1	12.6	48.1	9.8	1.8	8.9	1.4	8.1	1.5	3.8	0.6	3.7	0.6	40.8	251.1	7.8	9.4	0.6	0.9
16-FH-08	38.9	65.7	8.3	27.7	4.9	0.9	4.0	0.6	3.0	0.6	1.7	0.3	1.7	0.3	17.0	158.5	12.0	15.7	0.6	0.9
16-FH-09	47.0	86.1	9.9	35.0	7.0	1.4	6.9	1.0	6.1	1.2	3.0	0.5	3.1	0.5	31.4	208.9	8.4	10.3	0.6	0.9
16-FH-10	33.1	56.9	6.9	24.4	4.2	0.9	3.8	0.6	3.4	0.7	1.9	0.4	2.2	0.4	18.3	139.6	9.5	10.3	0.7	0.9
16-FH-11	29.6	56.9	6.8	23.4	4.6	0.9	4.2	0.6	3.6	0.7	1.9	0.3	2.1	0.3	18.8	135.8	8.9	9.7	0.6	0.9
16-FH-12	40.6	70.0	8.4	29.1	5.6	1.0	4.7	0.7	4.0	0.8	2.3	0.4	2.5	0.4	21.5	170.5	9.8	11.0	0.6	0.9
16-FH-13	54.6	113.5	12.9	48.1	11.9	2.8	12.7	1.7	9.2	1.7	3.9	0.6	3.7	0.6	39.0	277.8	7.2	10.0	0.7	1.0

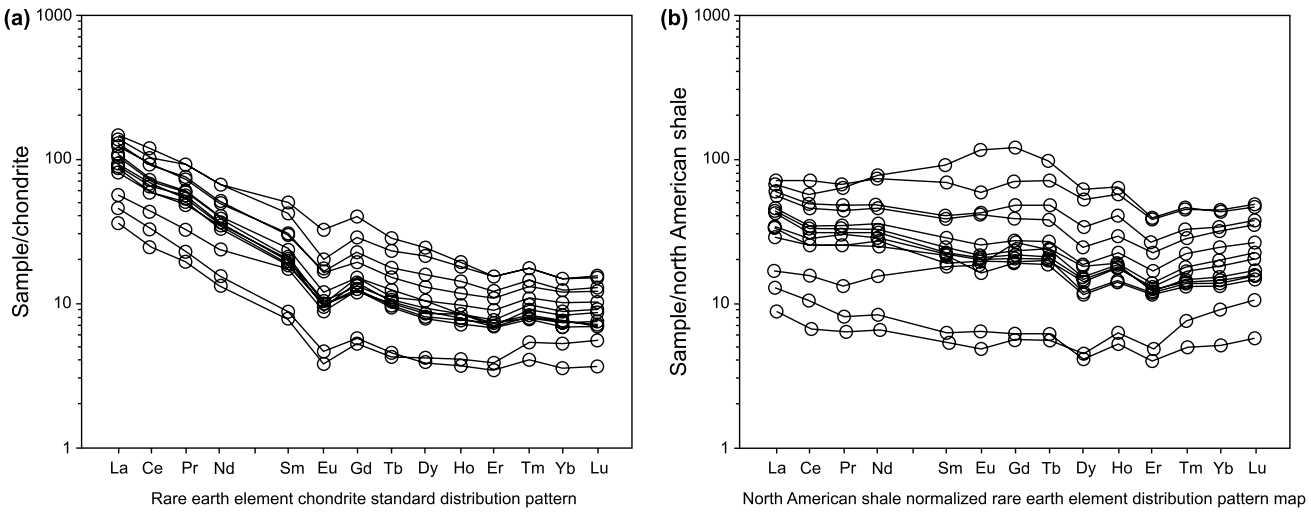

Fig. 6 Chondrite and North Americans shale-normalized REE distribution pattern of the Late Permian Dalong Formation mudstones. **a** Chondrite-normalized REE patterns; **b** North American shale-normalized REE patterns

earth element (∑REE) showed an increasing trend from top to bottom, indicating sedimentary water bodies became gradually shallower. At the same time, the maximum and minimum values of all samples were similar, reflecting the provenance of the parent rocks was the same. During the depositional period of the Dalong Formation (P_3d), the total content of rare earth elements (ΣREE) increased from top to bottom, indicating provenance was changed or differentiation occurred during the processes of sedimentation and diagenesis.

The content of the rare earth elements of all samples was allocated according to the chondrite standardization pattern and North American shale, and the results are shown in Fig. 6. The chondrite-standardized distribution pattern showed similar characteristics. The light rare earth elements were enriched, the distribution of heavy rare earth elements was regular, Eu showed a obviously negative anomaly and Ce showed a weak negative anomaly, indicating the paleo-water bodies were in a reducing environment (Calvert and Pedersen 1993; Algeo and Maynard 2004; Tribovillard et al. 2006). The results were consistent with the results revealed by the V/(V + Ni) ratio. The paleo-water body gradually deepened, and the water body in the lower part did not easily mix and certain stratification occurred. The ratio of ΣLREE/ΣHREE was in the range 6.3–11.8, showing a gradually decreasing trend, which indicated the sedimentary water bodies were strongly differentiated. The ratio of $(La/Yb)_N$ was between 7.0 and 15.7, with a mean value of 10.8, significantly higher than the value of PAAS (9.20), showing an increasing trend, which revealed strong differentiation

occurred in the rare earth elements in the paleo-water body. This was consistent with the phenomenon revealed by the stratigraphic section in the field geological survey. That was the reason the sand content increased from bottom to top. The ratio of $(La/Sm)_N$ and $(Gd/Yb)_N$ that could indicate the degree of differentiation of light and heavy rare earth elements was in the ranges of 4.60–8.62 and 1.73–2.42, with mean values of 6.92 and 2.14, respectively. The content of Eu appeared as a negative anomaly, in the range of 0.58–0.66, with a mean value of 0.62, lower than the Eu of PAAS (0.66).

4 Discussion

As discussed above, the paleo-water body in the Fenghai area, Fujian Province, experienced complicated oxidation–reduction processes during the depositional period of the Permian Dalong Formation. According to the variation of lithology, the content of sand increased from bottom to top, revealing the paleo-water depth became shallow. Moreover, corresponding geochemical characteristics also supported this result. However, what was the controlling factor? It will be discussed in the following part.

4.1 Tectonic environment discrimination of sedimentary water bodies

The geochemical characteristics of sedimentary rocks can reveal tectonic movement. Different provenances formed in different tectonic settings, corresponding to a unique sedimentary process. Although geochemical indexes depended on various conditions, unique geochemical indexes of sedimentary rocks, such as the variation of major elements, $Fe_2O_3 + MgO$, TiO_2 and Al_2O_3/SiO_2, and the variation of trace elements, Th, Sc, Co and Zr/10, can be used to distinguish the mudstone and sandstone formed in different areas and establish a geochemical discrimination diagram. These diagrams and a geochemical index are commonly used to evaluate sedimentary environments and tectonic backgrounds, such as oceanic arc, continental arc, active continental margin and passive continental margin (Bhatia 1983; Xie et al. 2015a, b; Gao et al. 2017).

Based on the characteristics of the major elements of ancient sandstone and mudstone and modern sandy mudstone, Roser and Korsch showed that K_2O/Na_2O and a K_2O/Na_2O–SiO_2 diagram could be used to effectively reflect the paleo-tectonic environment. The K_2O/Na_2O–SiO_2 diagram revealed that most analysis points were plotted into the area of passive continental margin, while minor analysis points were plotted into the area of active continental margin (Fig. 7). The result revealed that the tectonic background

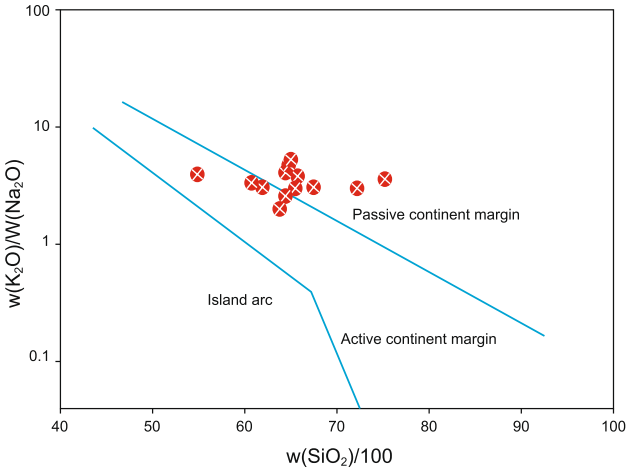

Fig. 7 Major elements indication of tectonic setting in the Permian Dalong Formation mudstone

of the provenance of the Permian Dalong Formation was passive continental margin.

The trace elements with high stability such as La, Th, Sc and Zr are not easily affected by weathering during transportation and diagenesis. Therefore, the geochemical indexes of trace elements can be used as indicators to study the types of sedimentary provenance and the tectonic setting (Bhatia and Taylor 1981; Bhatia and Crook 1986). After studying the trace elements of ancient graywacke from five known tectonic settings in eastern Australia, Bhatia and Crook showed that the fingerprints of trace elements were good indicators for tectonic settings and established a discrimination diagram of paleo-tectonic settings (Bhatia 1983; Bhatia and Crook 1986). From the triangular diagrams of La–Th–Sc and Th–Sc–Zr/10 established by Bhatia and Crook, it could be seen most samples were plotted into the continental margin (Fig. 8a, b). From the Th–Co–Zr/10 triangular diagram, it could be seen most samples were plotted into the continental margin and only a few samples were plotted into island arc (Fig. 8c). Thus, the provenance of the Dalong Formation (P_3d) was under a continental margin tectonic background (Fig. 8a–c), which was consistent with the results obtained from the major and trace elements.

4.2 Provenance attribute discrimination

The $w(K_2O)/w(Al_2O_3)$ ratio is significantly different for clay minerals and feldspar, so it is commonly used to determine the component of the provenance of fine-grained clastic rocks. Since mineral components were different in sediments, the ratio of $w(K_2O)/w(Al_2O_3)$ was also different for alkaline feldspar, illite and other clay minerals, among 0.4–0.1, ±0.3 and almost close to 0, respectively (Wronkiewicz and Condie 1987). The $w(K_2O)/w(Al_2O_3)$

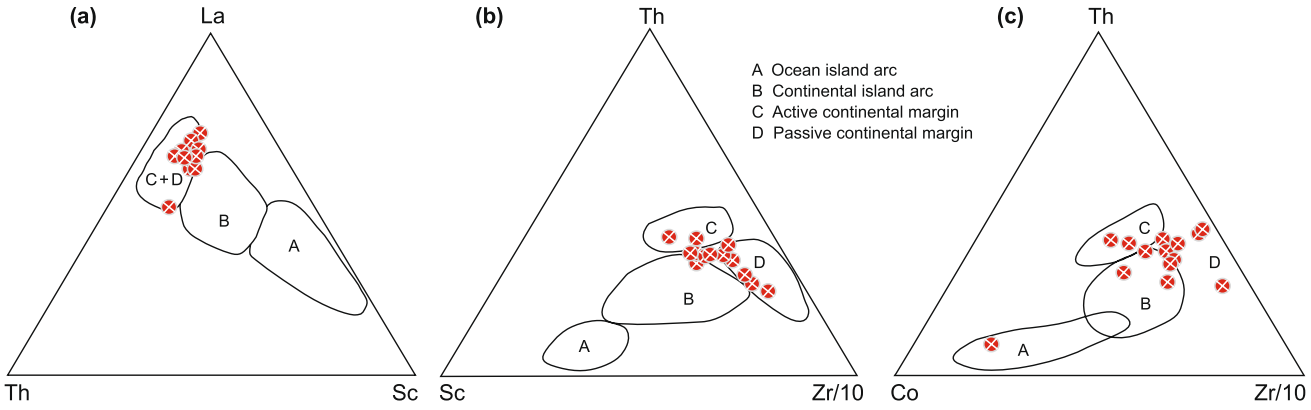

Fig. 8 Tectonic setting indication of trace elements in the Fenghai area. **a** La–Th–Sc discrimination diagram; **b** Th–Sc–Zr/10 discrimination diagram; **c** Th–Co–Zr/10 discrimination diagram. A—ocean island arc; B—continental island arc; C—active continental margin; and D—passive continental margin

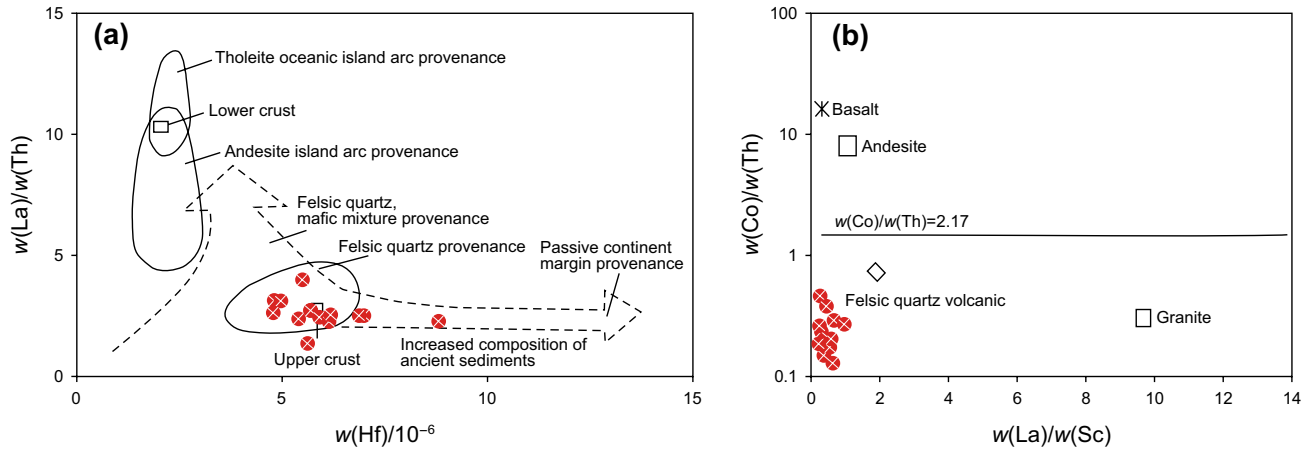

Fig. 9 Discrimination diagram for provenance attribute of the Late Permian Dalong Formation marine mudstone in the Fenghai area

ratio of argillaceous rocks reflected the content of alkaline feldspar in parent rocks. If it was less than 0.4, the content of alkaline feldspar was low, but if it was more than 0.5, the content of alkaline feldspar was high (Cox et al. 1995). The $w(K_2O)/w(Al_2O_3)$ ratio of the Permian Dalong Formation was between 0.04 and 0.22, with a mean value of 0.14, indicating the content of alkaline feldspar was low in the parent rocks. The results were consistent with the results obtained from the SiO_2–Al_2O_3 diagram (Figs. 3, 8).

The $w(K_2O)/w(Al_2O_3)$ ratio of sedimentary rocks was also an important indicator for the provenance of parent rocks. A value of less than 14 indicated the parent rocks might be mafic rocks (Girty et al. 1996). The value of 19–28 indicated the parent rocks might be granodioritic or quartz–mica–dioritic rocks (or andesitic and rhyolitic rocks) (Roser and Korsch 1986). The $w(K_2O)/w(Al_2O_3)$ ratio of the mudstone in the Dalong Formation (P_3d) was between 16.3 and 32, with a median value of 22.50 and a mean value of 23.7, indicating the provenance was derived from felsic and andesitic rocks. The results were consistent with results obtained in the lithological profile (the content of sand and SiO_2 was high).

At the same time, Co, Sc and Cr were more stable than La and Th and more easily enriched in acid rocks than basic rocks during the sedimentation period, which were also indicators for the provenance attributes (Roser and Korsch 1986; Girty et al. 1996). The mean values of Co/Th, La/Sc, Th/Sc and Th/Cr ratio were 0.46, 5.23, 2.02 and 0.16, respectively, similar to the corresponding characteristic ratios of continental upper crust (0.94, 2.70, 0.97 and 0.31), but significantly different from the characteristic ratios of continental lower crust and oceanic crust. Floyd et al. (1987) and Gu et al. (2002) proposed to discriminate provenance using w(La)/w(Th)–w(Hf) and w(Co)/w(Th)–w(La)/w(Sc) diagrams. The w(La)/w(Th)–w(Hf) diagram showed that the provenance was sourced from felsic volcanic rocks under a passive continental margin tectonic environment (Fig. 9a). w(Co)/w(Th)–w(La)/w(Sc) diagram showed that

w(Co)/*w*(Th) ratio was low in general, lower than 21.7, and the points were plotted into the region around felsic volcanic rocks (Fig. 9b). The results were consistent with the results obtained by major element, trace element and rare earth element.

The distribution patterns of rare earth elements are good indicators for provenance. When the provenance is from the upper crust, light rare earth elements are enriched, heavy rare earth elements are smoothly distributed and Eu shows a negative anomaly. The chondrite-standardized rare earth elements of the mudstone of the Dalong Formation (P_3d) are characterized by enriched light rare earth elements, flat distribution of heavy rare earth elements and an obvious Eu negative anomaly (Fig. 5a), similar to the distribution patterns of the rare earth elements in the upper crust, which revealed the provenance of the mudstone of the Dalong Formation was from the upper crust. The results are consistent with the results obtained by the characteristics of trace elements and diagram discrimination method.

4.3 Analyses of the sedimentary environment

The geochemical characteristics and the variation of major elements, rare earth elements and trace elements of the Dalong Formation (P_3d) revealed the same or similar results. During the depositional period of the Dalong Formation, the average content of SiO_2 was 64.7%, revealing an abundant supply of terrigenous materials. The content of Fe^{3+} in sediments was low, indicating a weakly oxidizing environment.

The chemical alteration index (f_{CIA}) is commonly used to determine the degree of chemical weathering in sedimentary provenance, which increases with the increase in the weathering degree of parent rocks (Nesbitt and Young 1982). The f_{CIA} value of the Late Permian Dalong Formation was in the range of 79.9–95.1 (Table 1), with a mean value of 85.6, indicating strong chemical weathering. The f_{CIA} value decreased from bottom to top in stratigraphic profile, indicating the degree of humidity and heat gradually decreased.

In sedimentary rocks, MgO is hydrophilic and Al_2O_3 is amphiphilic. Therefore, the magnesium and aluminum value (*b*) is often used to determine the salinity of paleo-water bodies (Wang and Luo 2009). Different *b* values correspond to different sedimentary environments. A *b* value of greater than 500 indicates an epicontinental environment (lagoon carbonate deposits), a *b* value between 50 and 100 indicates a marine environment, a *b* value between 1 and 10 indicated a marine–continental environment and a *b* value of less than 1 indicates freshwater (Wang and Luo 2009). The *b* value of the study area was in the range of 1.6–22.0, with an average value of 8.15 and a median value of 8.3 (Table 1), indicating the paleo-water bodies were in a semi-closed environment and the salinity was low.

The characteristics and discrimination diagram of rare earth elements and the ratios of V/Cr, Ni/Co, U/Th and Cu/Zn show the same or similar sedimentary environment. That was the reason abundant provenance was from an active continental margin, where paleo-water bodies were shallow, salinity increased and reducing conditions were strong. Moreover, transient delamination occurred during deposition.

5 Conclusions

(1) During the sedimentary period of the Dalong Formation (P_3d), the Fenghai region in southeastern Fujian Province was under an active continent margin or a passive continental margin tectonic environment.

(2) The ratio of major elements and the characteristics of minor and trace elements in Permian mudstone in Fenghai region showed the provenance was unaltered felsic rocks, which were dominated by potassium feldspar, with minor muscovite. The distribution pattern of rare earth elements was similar to that of the upper crust, characterized by enriched light rare earth elements, stably distributed heavy rare earth elements and an obviously negative Eu anomaly, indicating provenance was mainly derived from the upper crust and enriched.

(3) The characteristics of the trace elements of the Dalong Formation (P_3d) mudstone show that the sedimentary environment was neritic, where depositional rates gradually decreased, paleo-water bodies became shallow, the paleo-salinity gradually increased and the paleo-productivity increased. In addition, sedimentary water bodies showed occasional delamination.

Acknowledgements This article was supported by Opening Foundation of State Key Laboratory of Continental Dynamics, Northwest University; Opening Foundation of State Key Laboratory for Mineral Deposits Research, Nanjing University (20-15-05). We thank graduates Chen MJ, Gong Y, Wang XR et al., for their assistance in the geological surveying and also Zhu Q for his assistance with measurement. The authors are grateful to the Assistant Editor Jian Cao and the reviewers for commenting on the original draft and improvement to the manuscript.

References

Algeo TJ, Maynard JB. Trace element behavior and redox facies in core shales of Upper Pennsylvanian Kansas-type cyclothems. Chem Geol. 2004;206(3–4):289–318. https://doi.org/10.1016/j.chemgeo.2003.12.009.

Beek PV, Reyss JL, Bonte P, et al. Sr/Ba in barite: a proxy of barite preservation in marine sediments? Mar Geol. 2003;199(3–4):205–20. https://doi.org/10.1016/S0025-3227(03)00220-2.

Bhatia MR. Plate tectonics and geochemical composition of sandstone. J Geol. 1983;91(6):611–27. https://doi.org/10.1086/628815.

Bhatia MR, Crook KAW. Trace element characteristics of greywackes and tectonic discrimination of sedimentary basins. Contrib Miner Petrol. 1986;92:181–93. https://doi.org/10.1007/BF00375292.

Bhatia MR, Taylor SR. Trace element geochemistry and sedimentary provinces: a study from the Tasman geosyncline. Aust Chem Geol. 1981;33(1/2):115–25. https://doi.org/10.1016/0009-2541(81)90089-9.

Boulter CA, Hopkinson L, Ineson MG, et al. Provenance and geochemistry of sedimentary components in the volcano-sedimentary complex, Iberian Pyrite Belt: discrimination between the sill sedimentary complex and volcanic-pile models. J Geol Soc. 2004;161(1):103–15. https://doi.org/10.1144/0016-764902-159.

Calvert SE, Pedersen TF. Geochemistry of recent oxic and anoxic marine sediments: implications for the geological record. Mar Geol. 1993;113(1–2):67–88. https://doi.org/10.1016/0025-3227(93)90150-T.

Cao YC, Wang YZ, Xu TY, et al. Application of the ratio characteristic elements in provenance analysis: a case study from the upper part of the fourth member of the Shahejie Fm in the W58 area, Dongying depression. Acta Sedimentol Sin. 2007;25(2):230–8. https://doi.org/10.14027/j.cnki.cjxb.2007.02.010 **(in Chinese)**.

Cao J, Yang RF, Hu G, et al. Hydrocarbon potential of the Lower Cretaceous mudstones in coastal southeastern China. AAPG Bull. 2018;102(2):333–66. https://doi.org/10.1306/0503171617917074.

Cox R, Lower DR, Cullers RL. The influence of sediment recycling and basement composition on evolution of mud rock chemistry in the southwestern United State. Geochim Cosmochim Acta. 1995;59(14):2919–40. https://doi.org/10.1016/0016-7037(95)00185-9.

Cui YL, Xu H, Wang GH, et al. Geochemistry and genesis of the Bauxite Ore (Rock) in the Feichijiao ore district, Qiubei City, Yunnan Province. Acta Geosci Sin. 2017;38(3):372–84. https://doi.org/10.3975/cagsb.2017.03.07 **(in Chinese)**.

Duan JC. Sedimentological characteristics and hydrocarbon source rocks development regularity of the Mesozoic in Fujian and Zhejiang region. Beijing: China University of Geosciences; 2013. p. 1–55 **(in Chinese)**.

Dubini AV. Geochemistry of rare earth elements in the ocean. Lithol Miner Resour. 2004;39(4):289–97. https://doi.org/10.1023/B:LIMI.0000033816.14825.a2.

Elderfield H. The oceanic chemistry of rare-earth elements. Philos Trans R Soc Lond A Math Phys Eng Sci. 1988;325:105–16. https://doi.org/10.1098/rsta.1988.0046.

Feng HZ, Yu JH, Fang YT, et al. Another possible interpretation of Ce_{anom} for relative changes in paleo-oceanic redox conditions. J Nanjing Univ (Nat Sci). 1997;33(3):402–8. https://doi.org/10.3321/j.issn:0469-5097.1997.03.003 **(in Chinese)**.

Ferguson JE, Henderson GM, Kucera M, et al. Systematic change of foraminiferal Mg/Ca ratios across a strong salinity gradient. Earth Planet Sci Lett. 2008;15(1–2):153–66. https://doi.org/10.1016/j.epsl.2007.10.011.

Floyd PA, Leveridege BE. Tectonic environment of the Devonian Gramscatho basin, south Cornwall: framework mode and geochemical evidence from turbiditic sandstone. J Geol Soc. 1987;144(4):531–42. https://doi.org/10.1144/gsjgs.144.4.0531.

Gao LF, Zhou W, Zhang Y, et al. Geochemical characteristics of marine strata and the evolution of paleoceanographic environment from Late Jurassic to Early Cretaceous in Gonggar, Southern Tibet. Earth Sci Front. 2017;24(1):195–204. https://doi.org/10.13745/j.esf.2017.01.012 **(in Chinese)**.

Gardner JV, Dean WE, Vallier TL. Sedimentology and geochemistry of surface sediments, outer continental shelf, southern Bering Sea. Mar Geol. 1980;35(4):299–329. https://doi.org/10.1016/0025-3227(80)90123-1.

Girty GH, Ridge DL, Knaack C, et al. Provenance and depositional setting of Paleozoic chert and argillite, Sierra Nevada, California. J Sediment Res. 1996;66(1):107–18. https://doi.org/10.1306/D42682CA-2B26-11D7-8648000102C1865D.

Gu XX, Liu JM, Zheng MH, et al. Provenance and tectonic seeting of the Proterozoic turbidites in Hunan, South China: geochemical evidence. J Sediment Res. 2002;72(3):393–407. https://doi.org/10.1306/081601720393 **(in Chinese)**.

Han ZH, Wu B, Weng SF, et al. Geochemical characteristics of bauxite deposits in the Wh Chuan-Zheng'an-Daozhen area of Guizhou Province and their geological implications. Geol Explor. 2016;252(4):678–87. https://doi.org/10.13712/j.cnki.dzykt.2016.04.008 **(in Chinese)**.

Hatch JR, Leventhal JS. Relationship between inferred redox potential of the depositional environment and geochemistry of the Upper Pennsylvanian (Missourian) Stark Shale Member of the Dennis limestone, Wabaunsee County, Kansas, USA. Chem Geol. 1992;99(1-2-3):65–82. https://doi.org/10.1016/0009-2541(92)90031-Y.

Hu G, Hu WX, Cao J, et al. Source rock features and resource potential of the Lower Cretaceous strata in coastal Southeast China. Geol J China Univ. 2011;17(2):206–19. https://doi.org/10.16108/j.issn1006-7493.2011.02.007 **(in Chinese)**.

Hu G, Hu WX, Cao J, et al. Stratigraphic correlations and occurrence patterns of two sets of Lower Cretaceous black shales in coastal southeastern China and geological implications: insights from zircon U-Pb ages. Geol J. 2017a;52(4):594–608. https://doi.org/10.1002/gj.2813.

Hu G, Hu WX, Cao J, et al. The distribution, hydrocarbon potential, and development of the Lower Cretaceous black shales in coastal southeastern China. J Palaeogeogr. 2017b;6(4):333–51. https://doi.org/10.1016/j.jop.2017.08.002.

Hu XM, Wang JG, An W, et al. Constraining the timing of the India-Asia continental collision by the sedimentary record. Sci China Earth Sci. 2017c;60(4):603–25. https://doi.org/10.1007/s11430-016-9003-6.

Jiao YQ, Lu XB, Wang ZH, et al. Two distinct geological environments from sedimentary to diagenesis stages: examples from sandstones-type uranium deposits, Turpan-Hami Basin. Earth Sci J China Univ Geosci. 2004;29(5):615–20. https://doi.org/10.3321/j.issn:1000-2383.2004.05.018 **(in Chinese)**.

Li SJ, Xiao KH, Wo YJ, et al. REE geochemical characteristics and their geological signification in the Silurian, West of Hunan Province and North of Guizhou Province. Geoscience. 2008;22(2):273–80. https://doi.org/10.11781/sysydz201003262 **(in Chinese)**.

Liu YX, Hu WX, Hu G. Spores and pollen assemblages and their Paleo-climate implication from the Early Cretaceous dark mudstone in Zhejiang and Fujian Provinces. Geol J China Univ. 2014;207(4):590–601. https://doi.org/10.16108/j.issn1006-7493,2014.04.011 **(in Chinese)**.

McLennan SM. Rare earth elements in sedimentary rocks: influence of provenance and sedimentary processes. Rev Miner. 1989;21(8):169–200.

McManus J, Berelson WM, Klinkhammer GP, et al. Geochemistry of barium in marine sediments: implications for its use as a paleoproxy. Geochim Cosmochim Acta. 1998;62(21–22):3453–73. https://doi.org/10.1016/S0016-7037(98)00248-8.

Nesbitt HW, Young GM. Early Proterozoic climates and plate motions inferred from major element chemistry of lutites. Nature. 1982;299(5885):715–7. https://doi.org/10.1038/299715a0.

Pfeifer K, Kasten S, Hensen C, et al. Reconstruction of primary productivity from the barium contents in surface sediments of the South Atlantic Ocean. Mar Geol. 2001;177:13–24. https://doi.org/10.1016/S0025-3227(01)00121-9.

Roser BP, Korsch RJ. Determination of tectonic setting of sandstone-mudstone suites using SiO_2 content and K_2O/Na_2O ratio. J Geol. 1986;94:635–50. https://doi.org/10.1086/629071.

Shaw TJ, Gieskes JM, Jahnke RA. Early diagenesis in differing deposition environments: the response of transition metals in pore water. Geochim Cosmochim Acta. 1990;54:1233–46. https://doi.org/10.1016/0016-7037(90)90149-F.

Shaw TJ, Raiswell R, Hexel CR, et al. Input, composition, and potential impact of terrigenous material from free-drifting icebergs in the Weddell Sea. Deep Sea Res Part II Top Stud Oceanogr. 2011;58(11–12):1376–83. https://doi.org/10.1016/j.dsr2.2010.11.012.

Tang WX, Jiang ZX, Liu RH, et al. Geochemical characteristics and deposition environment of the Yogou Formation mudstone in the Termit Basin, Niger. Oil Gas Geol. 2017;38(3):592–602. https://doi.org/10.11743/ogg20170319 **(in Chinese)**.

Tribovillard N, Algeo TJ, Lyons T, et al. Trace metals as paleoredox and paleoproductivity proxies: an update. Chem Geol. 2006;232(1–2):12–32. https://doi.org/10.1016/j.chemgeo.2006.02.012.

Wagerich M, Neuhuber S. Stratigraphy and geochemistry of an Early Campanian deepening succession (Bibereck Formation, Gosau Group, Austria). Earth Sci Front. 2005;12(2):123–31. https://doi.org/10.3321/j.issn:1005-2321.2005.02.014 **(in Chinese)**.

Wang KM, Luo SS. Geochemical characteristics and environmental significance of Gaoyuzhuang and Yangzhuang Formation in Yanshan region. Bull Mineral Petrol Geochem. 2009;28(4):356–64. https://doi.org/10.3969/j.issn.1007-2802.2009.04.007 **(in Chinese)**.

Wright J, Schrader H, Holser TW. Paleoredox variations in ancient oceans recorded by rare earth elements in fossil apatite. Geochim Cosmochim Acta. 1987;51(3):631–44. https://doi.org/10.1016/0016-7037(87)90075-5.

Wronkiewicz DJ, Condie KC. Geochemistry of Archean shales from the Witwatersrand Supergroup, South Africa: source area weathering and provenance. Geochim Cosmochim Acta. 1987;51(9):2401–16. https://doi.org/10.1016/0016-7037(87)90293-6.

Xie XM, Hu WX, Cao J, et al. Preliminary investigation of depositional environment of black mud in Lower Cretaceous, Zhejiang and Fujian Provinces: micropaleontology and organic geochemical evidence. Acta Sedimentol Sin. 2012;28(6):1108–17. https://doi.org/10.14027/j.cnki.cjxb.2010.06.003 **(in Chinese)**.

Xie QF, Zhou LF, Cai YF, et al. Geochemistry and geological significance of the Permian mudstone in the South Qilian Basin, China. Bull Mineral Petrol Geochem. 2015a;34(2):354–61. https://doi.org/10.3969/j.issn.1007-2802.2015.02.24 **(in Chinese)**.

Xie QF, Zhou LF, Cai YF, et al. Geochemical characteristics of Permian marine source rocks and constraints of the provenance and paleoenvironment in the South Qilian Basin, Qinghai Province. Acta Geol Sin. 2015b;89(7):1288–301. https://doi.org/10.3969/j.issn.0001-5717.2015.07.011 **(in Chinese)**.

Xie QF, Cai YF, Dong YP, et al. LA-ICP-MS zircon U-Pb geochronology and Hf isotopic composition of Yanshanian granites in the Shanghang area, Fujian Province. Acta Geol Sin. 2017;91(10):2212–30. https://doi.org/10.3969/j.issn.0001-5717.2017.10.005 **(in Chinese)**.

Yang RF, Wang YC, Cao J. Cretaceous source rocks and associated oil and gas resources in the world and China: a review. Pet Sci. 2014;11(3):331–45. https://doi.org/10.1007/s12182-014-0348-z.

Yu Y, Zhang CM, Li SH, et al. Geochemical characteristics and geological significance of mudstone from the Zhujiang Formation of Huizhou depression. J China Univ Pet (Ed Nat Sci). 2014;38(1):40–9. https://doi.org/10.3969/j.issn.1673-5005.2014.01.006 **(in Chinese)**.

Zhang JL, Zhang X. The elemental geochemical features of ancient oceanic sedimentary environments in the Silurian period in the Tarim Basin. Period Ocean Univ China. 2006;36(2):200–8. https://doi.org/10.3969/j.issn.1672-5174.2006.02.005 **(in Chinese)**.

Zhang QM, Qin JH, Liao ZW, et al. Geochemical characteristics and material source of the Late Permian Bauxite deposits in Southeastern Yunnan Province. Geoscience. 2015;29(1):32–44. https://doi.org/10.3969/j.issn.1000-8527.2015.01.004 **(in Chinese)**.

Zheng RC, Liu MQ. Study of the palaeosalinity of the Chang 6 oil reservoir set in the Ordos basin. Oil Gas Geol. 1999;20(1):20–5. https://doi.org/10.11743/ogg19990105 **(in Chinese)**.